We are IntechOpen, the world's leading publisher of Open Access books Built by scientists, for scientists

6,900
Open access books available

185,000
International authors and editors

200M
Downloads

154
Countries delivered to

Our authors are among the

TOP 1%
most cited scientists

12.2%
Contributors from top 500 universities

BOOK CITATION INDEX
CLARIVATE ANALYTICS
INDEXED

WEB OF SCIENCE™

Selection of our books indexed in the Book Citation Index
in Web of Science™ Core Collection (BKCI)

Interested in publishing with us?
Contact book.department@intechopen.com

Mobile Sensors for Robotics Research

Tao Liu[1], Yoshio Inoue[1],
Kyoko Shibata[1] and Kouzou Shiojima[2]
[1]Kochi University of Technology
[2]TEC GIHAN Co., LTD
Japan

1. Introduction

Integrating rehabilitation robots with human motion and force sensors for effective training and positive therapeutic effects is attracting more and more attentions in research and clinic fields (Bonato, 2010; Moreno et al., 2009). In order to control robots at the level of human motor control, the muscular activity of the lower limbs which has been estimated from measurements of joint moments and segment orientations may be useful information for biomedical applications (Wu et al., 2009; Lin et al., 2010). Kinematic and kinetic data have been widely collected using a high-speed camera system and force plate for the estimation of lower limb joint loads in laboratory environments (Shakoor et al., 2010; Wannop et al., 2010). However, these commonly used stationary devices for human dynamics analysis require lots of space, special operators, expensive instruments and complex calibration settings; moreover, the range of measurement is limited to capturing a few strides in a gait laboratory. The main shortcomings restrict the application of these stationary devices to experimental research and it is difficult to find applications of gait evaluation in the daily environment or clinic. As an alternative to these conventional techniques, some inexpensive and easy to use wearable measurement systems which can accurately estimate triaxial ground reaction force (GRF) and three-dimensional (3D) body orientations have been developed to implement human dynamics analysis and gait assessments in different environments (Bachlin et al., 2010; Veltink et al., 2005) .

Recently, some inexpensive in-chip inertial sensors including gyroscopes and accelerometers have been gradually coming into practical application in human motion analysis. To expand the scope of application of a mobile force plate system, a small 3D inertial sensor module can be integrated into the force plate. Liedtke et al. proposed a combination sensor system including six degrees of freedom force and moment sensors and miniature inertial sensors (provided by Xsens Motion Technologies) to estimate the joint moments and powers of the ankle (Liedtke et al., 2007). If 3D orientations of the foot are obtained and integrated with measured triaxial GRF during gait, an inverse dynamic method can be used to implement joint dynamics analysis of the lower limb (Schepers et al., 2007).

We are presently concentrating on the development of some wearable sensors to measure human GRF and segment orientations during gait. A multi-axial force sensor has been developed to measure triaxial GRF and the coordinates of the center of pressure, when fixed under a specially designed shoe (Liu et al., 2007). However, its hard interface and the weight

load on the foot affected normal walking according to our experimental tests. A thin and light force plate based on 3D tactile sensors and using lower-cost materials was proposed in our past research (Liu et al., 2009a), and a sensor matrix will be constructed to directly perform triaxial GRF measurements. Moreover, in order to quantify human movements, we have developed some wearable sensor modules using gyroscopes and accelerometers for ambulatory measurements of human segment orientations (). In this chapter, a mobile force plate and 3D motion analysis system (M3D) is introduced, which have been reported in our former publication (Liu et al., 2010). 3D inertial sensor modules which were designed using lower cost inertial sensors including a triaxial accelerometer and gyroscope were integrated into a newly developed force plate. Verification experiments were conducted to compare the estimation results of M3D with measurements performed on a stationary force plate. Finally, an application experiment is introduced to quantify and evaluate human gait. We measured the 3D GRF and orientations of feet using M3D to evaluate paralysis gait

2. Methods and materials

2.1 Mechanical design of mobile force plate
Small triaxial force sensors (USL06-H5-500N) provided by Tec Gihan Co. Japan can only detect the three-directional force induced on a small circular plate (Φ 6 mm), see Table 1, so it is difficult to apply directly to the measurement of the GRF distributed under a foot. As shown in Fig. 1 (a), a mobile force plate (weight: 156g, size: 80×80×15mm3) was constructed using three small triaxial force sensors, in which two aluminum plates were used as top and bottom plates to accurately fix the three sensors. Each small sensor, when calibrated using data provided by the manufacturer, can measure triaxial forces relative to their slave coordinate systems ($\sum si$) defined on the center of each sensor, where subscript i represents the number of the small sensor in every force plate (i = 1, 2, and 3). The GRF and center of pressure (CoP) measured using the force plate so developed could be expressed in the force plate coordinate system ($\sum f$) which is located at the interface between the force plate and the ground, with the origin of the force plate coordinate system taken as the center of the force plate (see Fig. 1 (b)). The y-axis of the force plate coordinate system was chosen to represent the anterior-posterior direction of human movement on the bottom plate, and the z-axis was made vertical, while the x-axis was chosen such that the resulting force plate coordinate system would be right-handed. We aligned the y-axis of each sensor's slave coordinate to the origin of the force plate coordinate system, while the three origins of the slave coordinates were evenly distributed on the same circle (radius: r = 30 mm), and were fixed 120° apart from each other. Fxi, Fyi and Fzi were defined as the triaxial forces measured using the three triaxial sensors. The triaxial GRF and coordinates of the CoP could be calculated from the following equations:

$$F_x = (F_{x_1} + F_{x_3}) \cdot \cos(60°) - F_{x_2} - (F_{y_3} - F_{y_1}) \cdot \cos(30°) \tag{1}$$

$$F_y = (F_{y_1} + F_{y_3}) \cdot \cos(60°) - F_{y_2} - (F_{x_1} - F_{x_3}) \cdot \cos(30°) \tag{2}$$

$$F_z = F_{z_1} + F_{z_2} + F_{z_3} \tag{3}$$

$$M_x = F_{z_2} \cdot r - (F_{z_1} + F_{z_3}) \cdot \sin(30°) \cdot r \tag{4}$$

$$M_y = (F_{z_1} - F_{z_3}) \cdot \cos(30°) \cdot r \tag{5}$$

$$M_z = (F_{x_1} + F_{x_2} + F_{x_3}) \cdot r \tag{6}$$

$$x_{cop} = M_y / F_z \tag{7}$$

$$y_{cop} = M_x / F_z \tag{8}$$

$$z_{cop} = 0 \tag{9}$$

where *Fx, Fy* and *Fz* are defined as the triaxial GRF (F_{GRF}) measured using the force plate in the force plate coordinate system, and *Mx, My* and *Mz* indicate triaxial moments estimated from measurements of the three sensors, while x_{COP}, y_{COP} and z_{COP} are the coordinates of the CoP,

Small triaxial force sensors

(a)   (b)
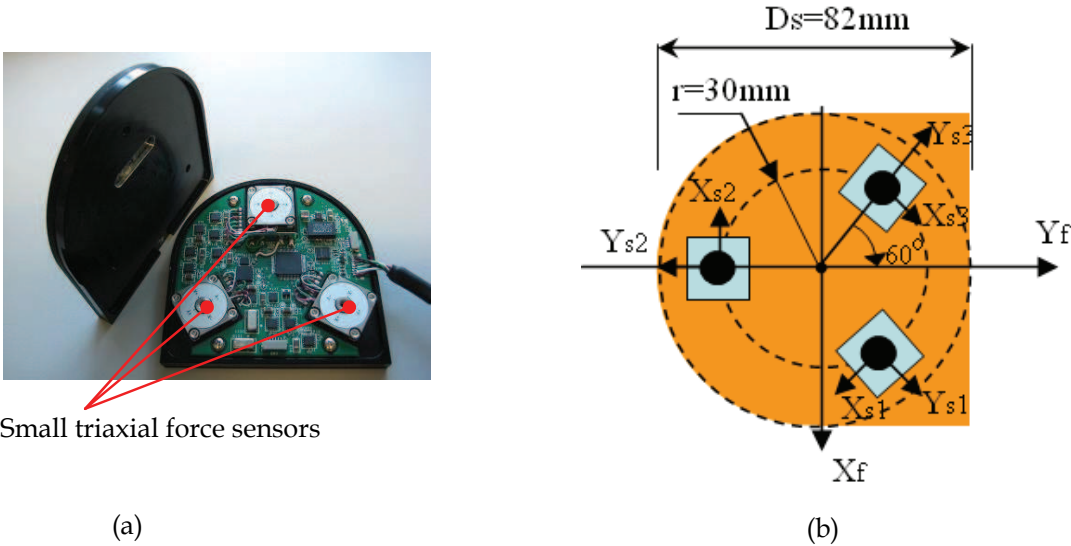
Fig. 1. (a) Prototype of a mobile force plate, (b) Coordinate systems of the force plate

Type		USL06-H5-500N
Rated Capacity (N)	X- and Y- axis	250
	Z-axis	500
Rated Capacity (με)	X- and Y- axis	900
	Z-axis	1700
Nonlinearity (After calibration of cross effect)		Within 1.0%
Hysteresis (After calibration of cross effect)		Within 1.0%
Size (mm)		20x20x5
Weight (g)		15

Table 1. Main specifications of the small triaxial force sensor used for the mobile force plate

In order to examine the inside force distribution of the mobile force plate, ANSYS FEA software was used to perform a static analysis and to simulate the effects of multi-axial

forces which may be distributed over the three contact points of the small sensors on the top aluminum plate.

Fig. 2 shows the finite element mesh and a representative result of the deformation of the top plate which is attached to the small sensors using three M3 screws. When we load the top plate with a z-axial force Fz = 733.57 N (vertical pressure: 0.125 MPa) and y-axial force Fy = 263.5 N (spread over 527 nodes), and x-axial force Fx = 263.5 N (spread over 527 nodes), the induced three-directional forces on the small sensor can be calculated by the finite element method and the results are given in Table 2. The maximum force (274.6 N) on the z-axis of the three sensors, and the maximum x- and y-axis forces of 136.61 N never exceed the measurement capacity of the small sensor.
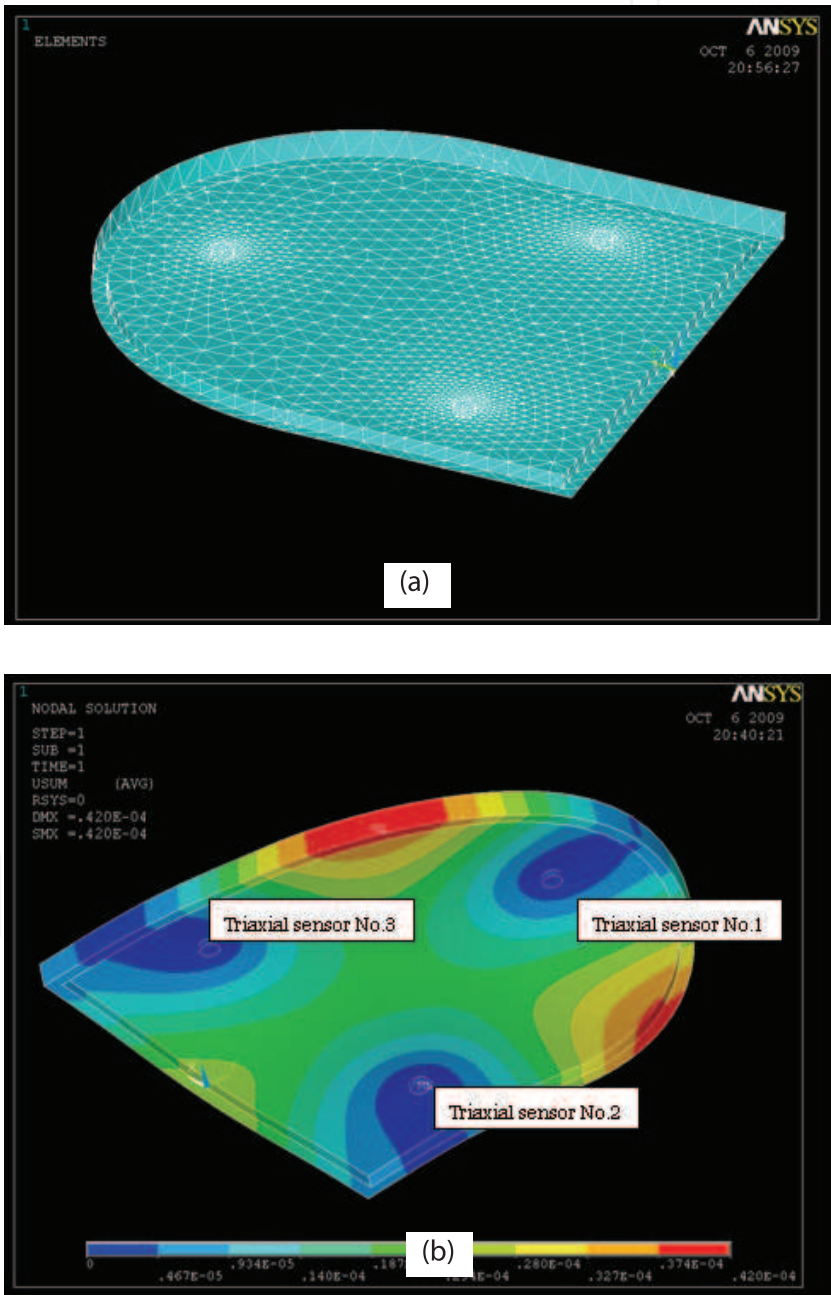
Fig. 2. (a) Finite element mesh, (b) Results of deformation plot

No.	Triaxial Forces (N)		
	X	Y	Z
1	89.48	136.61	274.6
2	59.19	69.03	219.7
3	114.83	58.16	239.27

Table 2. Three-directional forces on the small sensor when we load the force plate by Fz= 733.57N, Fy=263.5N and Fx=263.5N

2.2 Estimation of 3D orientation

As shown in Fig. 3, we constructed a 3D motion sensor module composed of a triaxial accelerometer (MMA7260Q, supplied by Sunhayato Co.) and three uniaxial gyroscopes (ENC-03R, supplied by Murata Co.) on the PCB board inside the mobile force plate. The module can measure triaxial accelerations and angular velocities which can be used to estimate a 3D orientation transformation matrix, so we can implement ambulatory GRF and CoP measurements using the combined system of mobile force plate and 3D motion analysis system (M3D).

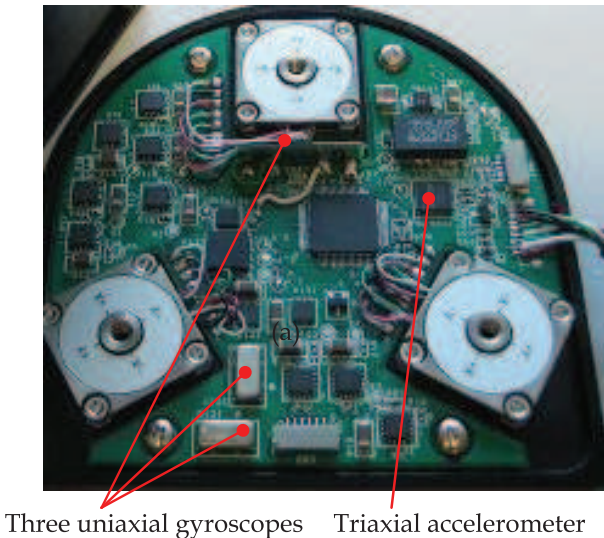Three uniaxial gyroscopes   Triaxial accelerometer

Fig. 3. 3D motion sensor module constructed using three uniaxial gyroscopes and a triaxial accelerometer

We defined two local coordinate systems fixed to the two M3Ds under the heel and the forefoot as $\sum_{f\_heel}$ and $\sum_{f\_toe}$ respectively (see Fig. 4). The relative position of the two force plates was aligned using a simple alignment mechanism composed of three linear guides and a ruler to let the origins of $\sum_{f\_toe}$ be on the y-axis of $\sum_{f\_heel}$, and to let the y-axes of the two force plate coordinate systems be collinear, before we mounted them to a shoe. For calculation purposes, such as estimating joint moments and reaction forces of the ankle during loading response and terminal stance phases (Parry, 1992), all vectors including the joint displacement vector, GRF vector and gravity vector have to be expressed in the same coordinate system, that is the global coordinate system ($\sum_g$). Moreover, the origin and orientation of this global coordinate system are renewed for each foot placement to coincide with the heel force plate coordinate system ($\sum_{f\_heel}$), when the heel is flat on the ground.

The integration of the measured angular velocity vector ($\omega = [\omega x, \omega y, \omega z]$) in each force plate coordinate system was defined as $C = [Cx, Cy, Cz]$, which could be used to calculate the 3D

orientation transformation matrix (R) between the global coordinate system and a force plate coordinate system by solving the following equations proposed by Bortz (1970):
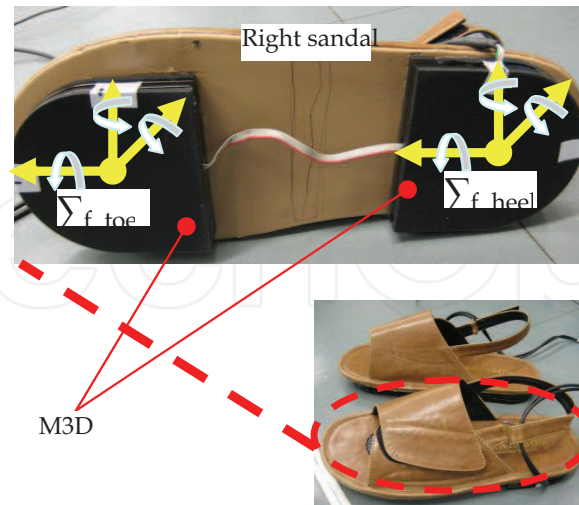

Fig. 4. M3D and the coordinate systems

$$C_i^{i+1} = [\omega x(i) + \omega x(i+1), \omega y(i) + \omega y(i+1), \omega z(i) + \omega z(i+1)] \cdot (\Delta t / 2) \tag{10}$$

$$\left|C_i^{i+1}\right| = \sqrt{(Cx_i^{i+1})^2 + (C_{yi}^{i+1})^2 + (Cz_i^{i+1})^2} \tag{11}$$

$$R_i^{i+1} = \frac{C_i^{i+1} \cdot C_i^{i+1^T}}{\left|C_i^{i+1}\right|}(1 - \cos\left|(C_i^{i+1})\right|) + \begin{bmatrix} \cos\left|(C_i^{i+1})\right| & 0 & 0 \\ 0 & \cos\left|(C_i^{i+1})\right| & 0 \\ 0 & 0 & \cos\left|(C_i^{i+1})\right| \end{bmatrix}$$

$$+ \frac{\sin(\left|C_i^{i+1}\right|)}{\left|C_i^{i+1}\right|}\begin{bmatrix} 0 & -C_{z_i^{i+1}} & C_{y_i^{i+1}} \\ C_{z_i^{i+1}} & 0 & -C_{x_i^{i+1}} \\ -C_{y_i^{i+1}} & C_{x_i^{i+1}} & 0 \end{bmatrix} \tag{12}$$

$$R = R_0 \cdot R_0^1 \cdot R_1^2 \cdot\cdot R_i^{i+1} \cdots \tag{13}$$

where $[\omega x(i), \omega y(i), \omega z(i)]$ is a sample vector of the triaxial angular velocities of the force plate during a sampling interval Δt, $Cii+1$ is an angular displacement vector in the sampling interval, and $R0$ is an initial transformation matrix initialized as a unit matrix ($|R_0|$=1). If the force plate is flat on a level ground, we can update R according to $R = R_0$.

2.3 Transformation of triaxial GRF measured by mobile force plates
The triaxial GRF measured by the two M3Ds can be transformed to global coordinates and then combined to calculate the total GRF (F_{FRG}^g) and the global coordinate vectors of CoP ($[x,y,z]_{COP}^{g\_heel}$ and $[x,y,z]_{COP}^{g\_toe}$) using the following equations:

$$F_{FRG}^{g} = R_{g}^{f-heel} \cdot F_{FRG}^{heel} + R_{g}^{f-toe} \cdot F_{FRG}^{toe} \tag{14}$$

$$[x,y,z]_{COP}^{g-heel} = R_{g}^{f-heel} \cdot [x,y,z]_{COP}^{heel} \tag{15}$$

$$[x,y,z]_{COP}^{g-toe} = R_{g}^{f-toe} \cdot [x,y,z]_{COP}^{toe} \tag{16}$$

where F_{FRG}^{heel} and F_{FRG}^{toe} are the triaxial GRF measured by the two M3Ds under the heel and forefoot with their respective coordinate systems; $[x,y,z]_{COP}^{heel}$ and $[x,y,z]_{COP}^{toe}$ are coordinate vectors of CoP measured using the two M3Ds; R_{g}^{f-heel} and R_{g}^{f-toe} are the orientation transformation matrices of the two M3Ds for transforming the triaxial GRF measured by the two M3Ds in their attached coordinate systems into the measurement results relative to the global coordinate system.

3. Experimental study

3.1 Verification experiment

A stationary TF-4060-A force plate (Tec Gihan Co. Japan) was used as a reference measurement system to verify the measurement results of the M3D system being developed. As shown in Fig. 5, a young volunteer wearing M3D was asked to walk on the stationary force plate and the signals from the two measurement systems were simultaneously sampled at a rate of 100 samples/s, after a trig signal was sent from the data logger of the M3D.

First, a static test experiment was conducted to validate the triaxial force measurement of the M3D without movement. Only one foot wearing the M3D is put on the stationary force plate and the subject arbitrarily moved his center of pressure. As shown in Fig. 6, the triaxial measurement results obtained with the stationary force plate (FP) and M3D almost completely overlap and the maximum errors in the triaxial force measurements were less than 5% of the corresponding maximum forces. Second, in order to verify the M3D ambulatory measurement, a dynamic test was performed on a walking measurement, in which the subject was asked to step on the force plate at a normal speed of about one step/s (see Fig. 7). The verification experiment results indicate that the sensor can measure the triaxial force with high precision (error: less than 6.4% of the maximum measurement force) under static and dynamic working conditions.

3.2 Measurement of paralysis gait using M3D

I As an application of the research, experiments were performed to quantitatively compare and analyze normal walking and paralysis walking using the M3D. The main features of paralysis gait can be summarized as follows: the toe on the paralyzed side rotates to the outside with a larger angle than in normal gait; the knee is stretched to the outside during the swing phase. A healthy subject was trained to imitate the walking feature of paralysis, and we separately measured the imitated paralysis gait of the left leg and right leg. The walking distance of the experimental tests is about 6 m.

Figs. 8 and 9 give the vertical components of GRF on the two feet (Solid blue line: GRF on the left foot; Solid pink line: GRF on the right foot) measured with the M3D system in normal gait and on the right foot imitating paralysis gait, respectively. We note that there are no large differences in the shape of the vertical force (z-axial force) curves induced on
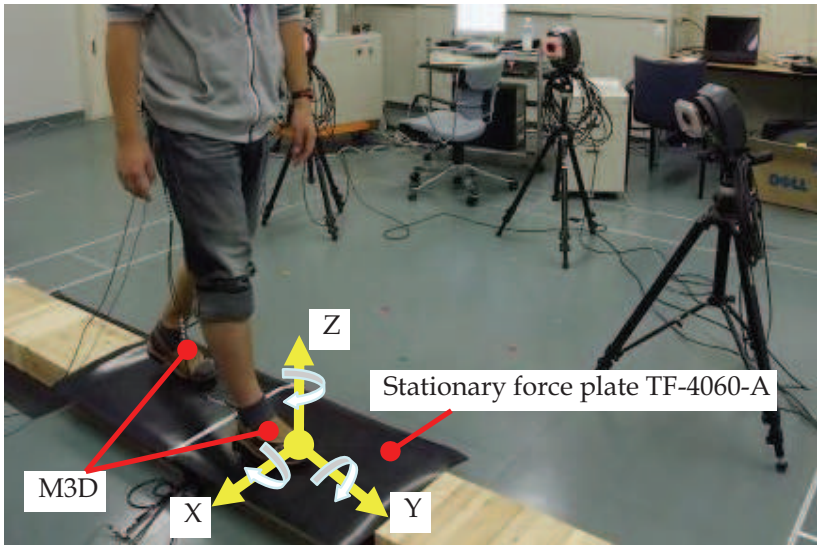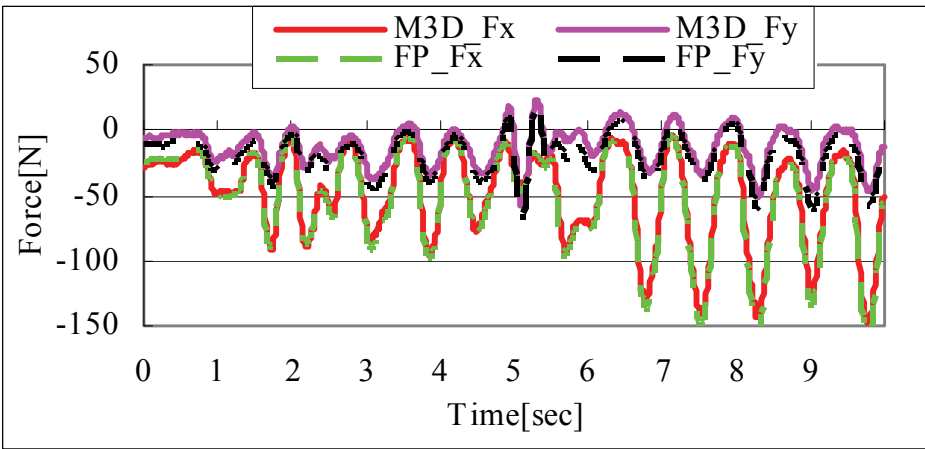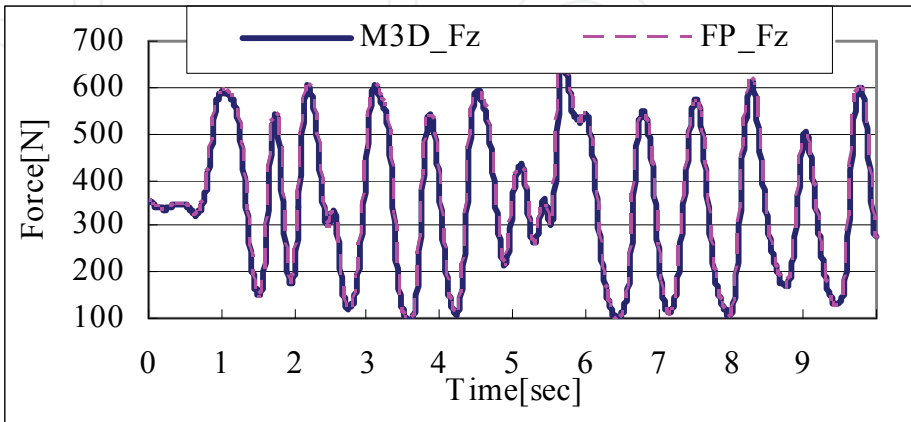
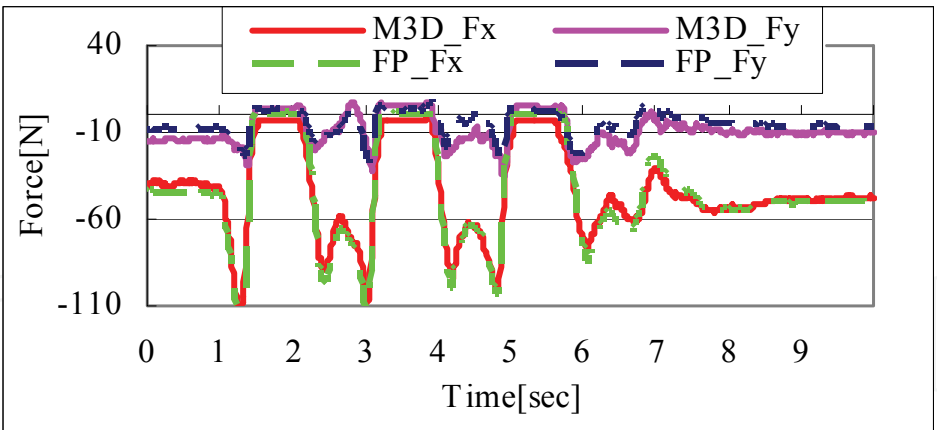Fig. 5. Verification experiments to validate the measurements of the M3D

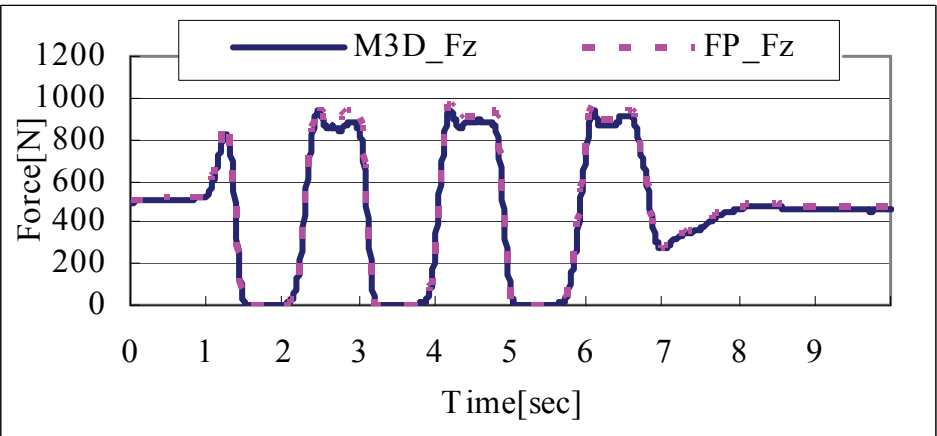(a) X and Y - axial forces when standing on the stationary force plate

(b) Z-axial force when standing on the stationary force plate

Fig. 6. Experiment results of the static test

(a) X and Y - axial forces when stepping on the stationary force plate

(b) Z-axial force when stepping on the stationary force plate

Fig. 7. Experiment results of the dynamic test

the right and left foot during normal walking, and that the GRF on the two feet have good balance and symmetry during continuous strides. When we compare the curves in Fig. 9 with the normal gait data, we can clearly note that the two peaks of the z-axial force on the left foot which is not on the paralyzed side are depressed. Moreover, it has been understood that the stance phase period of the healthy leg (the left leg) was about 1.6 times longer than the paralyzed side (the right leg) during a stride.

The rotation angles of the toe and heel of the feet around the medial-lateral direction (x-axis, see Fig. 5) are shown in Fig. 10, in which the dotted lines indicate the movements of the right foot and the rotation angles of the left foot are plotted with solid lines. The positive angle values represent the plantar flexion of the foot segments, and the negative values indicate dorsal flexion. The flexion angles of the paralysis foot (the right foot) are reduced significantly and the heel-strike angles and toe-off angles were less than 20 degrees. Moreover, it is noted that the toe joint of the paralysis foot was almost never rotated during the gait, because the heel and toe had the same flexion angles during the entire walking measurements. We also obtained similar results in the measurements of left leg paralysis using the M3D.
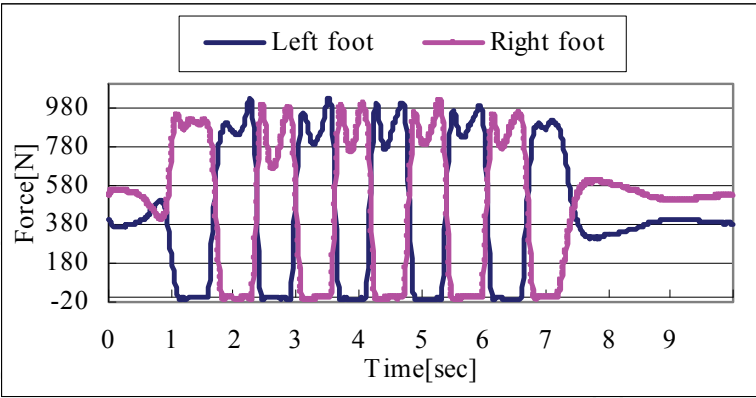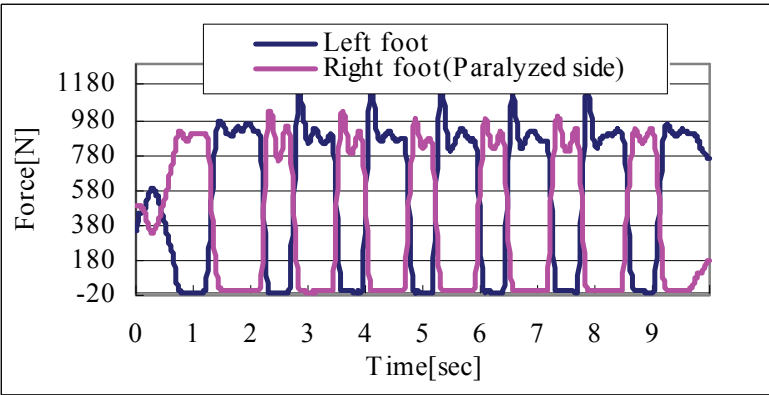
Fig. 8. Z-axis force during normal walking

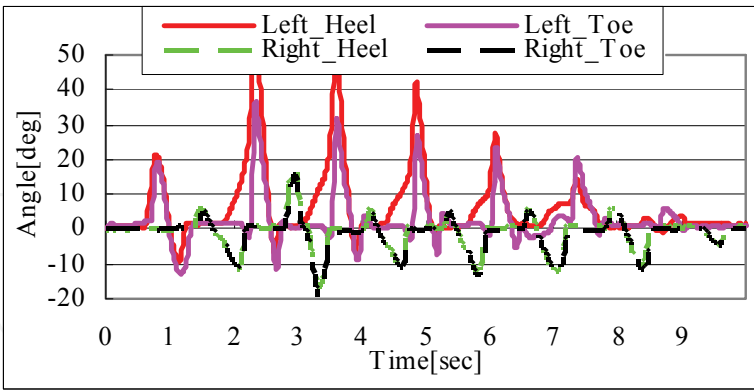

Fig. 9. Z-axis force during paralysis gait

Fig. 10. X-axial angles of the feet during paralysis gait

4. Discussions and conclusions

A mobile force plate and 3D motion analysis system (M3D) was developed using lower cost inertial sensor chips and small triaxial force sensors. In order to apply the system to human gait evaluation, verification experiments were implemented to compare the results estimated by M3D with measurements made with a stationary force plate. In the static tests, the force measurements by the M3D system along three axes were highly correlated in both

amplitude and dynamic response to the reference measurements using the stationary force plate (see Fig. 6) and this verifies that the M3D system could measure the triaxial GRF in its fixed local coordinate system with acceptable precision (less than 5% of the corresponding maximum force). However, as shown in Fig. 7, there were larger errors in the triaxial GRF measurements. The most likely source of amplitude error in the triaxial GRF measurement was in the orientation estimate of M3D movements using a triaxial accelerometer which could only implement x- and y-axial angular displacement re-calibration. In the future, we will integrate a triaxial magnetic sensor (Zhu & Zhou, 2009) for estimating the heading angle (z-axial angular displacement) during gait, because the z-axial (vertical) cumulative error induced by the drift effect of the gyroscope sensor could be re-calibrated using measurements from the magnetic sensor. Since only straight level walking was tested with M3D, it is necessary to examine more movements to verify ambulatory measurements obtained with M3D in future gait experiments. Moreover, the sensitivity of results to initial sensor drift and initial orientation fix will be addressed so that the system can be applied to many other applications.

In our research application using the new system, the quantitative differences between paralysis gait and normal gait were analyzed based to the results of z-axial GRF (Fig. 9) and x-axial angular flexions (Fig. 10). In clinical applications, the quantitative analysis of gait variability using kinematic and kinetic characterizations can be helpful to medical doctors in monitoring patient recovery status. Moreover, these quantitative results may help to strengthen their confidence in rehabilitation. Walking speed, stride length, center of mass (CoM) and CoP have been considered as influencing factors in evaluations of human gait (Lee & Chou, 2006). In this paper, only the z-axial GRF (vertical force) and x-axial orientation were analyzed to evaluate different gaits. However, according to one study on slip type falls (Chang et al., 2003), the friction force was used to draw up important safety criteria for detecting safe gait, so the transverse components of GRF may provide important information when quantifying gait variability. The M3D system can be used to obtain multi-dimensional motion and force data on successive gait in non-laboratory environments, so we will develop a new method based on measurements from the mobile system for quantifying gait variability. Moreover, a statistical analysis of the multi-dimensional GRF and orientation data extracted from successive gait measurements will be used to evaluate normal and pathological gait.

5. References

Bonato, P. (2010). Wearable sensors and systems, *IEEE Engineering in Medicine and Biology Magazine*, 29 (3), pp. 25-36.

Bachlin, M.; Plotnik, M.; Roggen, D.; Maidan, I.; Hausdorff, J.M.; Giladi, N. & Troster, G. (2010). Wearable assistant for Parkinsons disease patients with the freezing of gait symptom, *IEEE Transactions on Information Technology in Biomedicine*, 14 (2), pp. 436-446.

Bortz, E. (1970). A new mathematical formulation for strapdown inertial navigation, *IEEE Trans. Aero. Ele.,* 7(1), pp.61-66.

Chang, W.R.; Courtney, T. K. ; Gronqvist, R. & Redfern, M.S. (2003). *Measuring slipperiness: human locomotion and surface factors*, CRC Press, Chapter 1.

Lee, H.J. & Chou, L.S. (2006). Detection of gait instability using the center of mass and center of pressure inclination angles, *Archives of Physical Medicine and Rehabilitation*, 87, pp.569-575.

Liedtke, C.; Fokkenrood, W.; Menger, T.; van der Kooij, H. & Veltink, H. (2007). Evaluation of instrumented shoes for ambulatory assessment of ground reaction forces, *Gait and Posture*, 26(1), pp.39-47.

Lin, Y.C.; Walter, J.P.; Banks, S.A.; Pandy, M.G. & Fregly, B.J. (2010). Simultaneous prediction of muscle and contact forces in the knee during gait, *Journal of Biomechanics*, 43 (5), pp. 945-952.

Liu, T.; Inoue, Y. & Shibata, K. (2007). Wearable Force Sensor with Parallel Structure for Measurement of Ground-reaction Force, *Measurement*, 40(6), pp.644-653.

Liu, T.; Inoue, Y. & Shibata, K. (2009a). A Small and Low-cost 3D Tactile Sensor for a Wearable Force Plate, *IEEE Sensors Journal*, 9(9), pp.1103-1110.

Liu, T.; Inoue, Y. & Shibata, K. (2009b). Development of a Wearable Sensor System for Quantitative Gait Analysis, *Measurement,* 42(7), pp. 978-988.

Liu, T.; Inoue, Y.; Shibata, K.; Hirota, Y. & Shiojima K. (2010). A Mobile Force Plate System and Its Application to Quantitative Evaluation of Normal and Pathological Gait, *Proceedings of IEEE/ASME International Conference on Advanced Intelligent Mechatronics*, Montreal, Canada.

Moreno, J.C.; Brunetti, F.; Navarro, E.; Forner-Cordero, A. & Pons, J.L. (2009). Analysis of the human interaction with a wearable lower-limb exoskeleton, *Applied Bionics and Biomechanics*, 6 (2), pp. 245-256.

Parry, J. (1992). *Gait analysis normal and pathological function, Slack Incorporated*, pp.149-158.

Schepers, M.; Koopman, M. & Veltink, H. (2007). Ambulatory assessment of ankle and foot dynamics, *IEEE Trans. Biomed. Eng.*, 54(5), pp.895-900.

Shakoor, N.; Sengupta, M.; Foucher, K.C.; Wimmer, M.A.; Fogg, L.F. & Block, J.A. (2010). Effects of common footwear on joint loading in osteoarthritis of the knee, *Arthritis Care and Research*, 62 (7), pp. 917-923.

Veltink, H.; Liedtke, C.; Droog, E. & Kooij, H. (2005). Ambulatory measurement of ground reaction forces, *IEEE Trans Neural Syst Rehabil Eng.*, 13(3), pp.423–527.

Wannop, J.W.; Worobets, J.T. & Stefanyshyn, D.J. (2010). Footwear traction and lower extremity joint loading, *American Journal of Sports Medicine*, 38 (6), pp. 1221-1228.

Wu, J.Z.; Chiou, S.S. & Pan, C.S. (2009). Analysis of musculoskeletal loadings in lower limbs during stilts walking in occupational activity, *Annals of Biomedical Engineering*, 37(6), pp.1177-1189.

Zhu, R. & Zhou, Z. (2009). A small low-cost hybrid orientation system and its error analysis, *IEEE Sensors Journal,* 9(3), pp.223-230.

Biped Robots

Edited by Prof. Armando Carlos Pina Filho

Biped robots represent a very interesting research subject, with several particularities and scope topics, such as: mechanical design, gait simulation, patterns generation, kinematics, dynamics, equilibrium, stability, kinds of control, adaptability, biomechanics, cybernetics, and rehabilitation technologies. We have diverse problems related to these topics, making the study of biped robots a very complex subject, and many times the results of researches are not totally satisfactory. However, with scientific and technological advances, based on theoretical and experimental works, many researchers have collaborated in the evolution of the biped robots design, looking for to develop autonomous systems, as well as to help in rehabilitation technologies of human beings. Thus, this book intends to present some works related to the study of biped robots, developed by researchers worldwide.

How to reference

In order to correctly reference this scholarly work, feel free to copy and paste the following:

INTECH
open science | open minds